Revue des Composites et des Matériaux Avancés-Journal of Composite and Advanced Materials
Vol. 35, No. 2, April, 2025, pp. 303-310
Journal homepage: http://iieta.org/journals/rcma

Finite Element Analysis of the Radial Cracks at Glass Fiber Rinforced Polymer (GFRP) Reinforced Concrete: Effect of the Concrete Hydration Process

Ahlem Sdiri[1*], Slim Kammoun[2], Atef Daoud[1]

[1] Research Unit "Geomaterials, Structures in Civil Engineering and Environment" (GESTE), National Engineering School, University of Sfax, Sfax 3038, Tunisia
[2] Laboratory of Civil Engineering, National School of Engineering of Tunisia (ENIT), University of Tunis El Manar, Tunis 1002, Tunisia

Corresponding Author Email: ahlem.sdiri@yahoo.com

https://doi.org/10.18280/rcma.350212

Received: 5 February 2025
Revised: 6 March 2025
Accepted: 22 March 2025
Available online: 30 April 2025

Keywords:
concrete, damage (GFRP), FE

ABSTRACT

This study presents a numerical analysis of the occurrence of radial damage in concrete reinforced with glass fiber-reinforced polymer (GFRP) rebars. The difference in radial thermal expansion coefficients between GFRP rebars and concrete can induce cracking in the surrounding concrete. Furthermore, the behavior of early-age concrete is significantly influenced by the hydration process, which was simulated using the finite element software ABAQUS. Numerical simulations were conducted to assess the evolution of cracking in early-age concrete reinforced with GFRP rebars. The thermal strain, dependent on the degree of hydration, was incorporated into the simulation. The temperature evolution due to the heat of hydration was also modeled, with peak hydration temperatures reaching approximately 50°C, to capture the development of thermal gradients in the concrete. Mazar's damage model was employed to describe radial cracking. An analytical model was applied to study early-age concrete, wherein its thermo-mechanical properties were defined as functions of the hydration degree. Numerical results reveal that radial damage in early-age concrete is particularly pronounced around GFRP reinforcement. A comparison of the numerical results with analytical solutions confirms the validity of the model, with relative error of 8.57×10^{-6} highlighting the accuracy of the proposed numerical approach.

1. INTRODUCTION

The early age concrete is characterized by a thermo-chemical process which depends on the cement's hydration. Subsequently, the durability of structures depends mainly on these thermo-chemical evolutions [1, 2]. The hydration process is quantified by the hydration degree ξ [3, 4]. In fact, it is considered as an important parameter which describes the concrete's hardening during. This consecutive chemical reaction leads to the increase of the concrete 's temperature. It may reach up to 60°C [5-7]. This justifies its exothermal character. Hence, the temperature variation leads to the appearance of the thermal shrinkage [8, 9]. This phenomenon presents a source of cracking appearance in early age concrete [5].

For cementitious materials, microstructure evolution plays an important role in the bonding properties of the concrete [10]. Chemically, various analytical and numerical models have been developed to study the cement hydration evolution depending on the external temperature and the composed concrete type. As example, The HYMOSTRUC [11] model was elaborated by Ye et al. [11] and it is used to simulate the hydration process and to evaluate the pore structure characteristics in the concrete paste. Furthermore, depending on the cement compositions (Silica SiO_2, Alumina Al_2O_3, Lim Cao etc.), the variation of the variation degree as function of time is determined. For CEMHYD3D model [12], for a giving water cement ratio, the cement particles are modelled as a continuity of spheres with different diameters. the cement hydration process is simulated as the growth of the cement particles. Moreover, it was proven that the early age concrete proprieties depend mainly on the hydration degree according to analytical and experimental study elaborated by De Schutter and Taerwe [13]. The problem of cracks appearance on early age concrete is related to the attain of the concrete's stress to the maximum concrete's tensile strength. Hence, this fact leads to various problem in the structures notably the steel's rebars corrosion. In fact, it may lead to the degradation of the concrete interface around the rebar of reinforcement. In order to prevent such problem, an alternative technology of reinforcement is recently used which is the composite rebars (FRP) in particular the (GFRP ones) [14, 15]. In fact, these rebars are performed by their non-corrosive aspect and their lightweight [16-18]. Sdiri et al. [5] elaborated a finite element analysis of early age concrete reinforced with (GFRP) elements. In this model, the hydration degree was taken in

account to determine the cracks evolution in the concrete specimen. Besides, a numerical comparative has been deduced between Steel and GFRP reinforcements at early age concrete. It was proven that the use of the GFRP rebars minimizes the transversal cracks appearances [5]. Moreover, this composite materials present, in the glass fibers direction, a thermal coefficient (CET) equal to the concrete one. Perhaps, they are characterized by a coefficient of thermal expansion (CET) more important to the concrete one ((CET GFRP=2-3CETconcrete) [19, 20]. This Caracter leads to the appearance of radial cracks in the hardened concrete. The GFRP character has been exploited in various experimental, analytical and numerical simulations to study the case of hardened concrete reinforced with GFRP rebar [20, 21]. Zaidi et al. [20] developed an experimental and analytical study in which they considered a cylindrical hardened concrete beam reinforced with GFRP rebar and exposed to various thermal loads. As results, it is deduced analytically the radial pressure applied by the composite rebar on the concrete [20, 21]. Subsequently, the radial concrete's stresses are expressed and deduced as functions of the thermos-mechanical concrete and rebar's proprieties. Ones the radial concrete's stress attempt its maximal tensile strength, radial cracks would appear around the GFRP rebar. Furthermore, it was proven that radial cracks occur in concrete at FRP bar/concrete interface at a temperature variation of 20 to 25°C [20]. Perhaps, the number of research studies related to the thermal effect on GFRP bars embedded in early age concrete is very limited. Hence, the thermal strain distributions at the interface GFRP–bar/ surrounding early age concrete need to be further investigated.

Although numerous studies have examined the bond performance of GFRP bars in concrete, most of the existing research has primarily focused on the long-term behavior of GFRP-reinforced concrete or fully matured concrete conditions [21-23]. However, limited attention has been given to understanding the bond behavior of GFRP reinforcement at early ages, particularly under varying curing conditions. Early-age bond performance is crucial for ensuring structural integrity during the initial stages of construction, especially when accelerated construction techniques such as steam curing are applied.

Recent studies have investigated the bond characteristics of GFRP bars in different cementitious composites [24, 25], and the cracking behavior of GFRP-reinforced concrete at early ages [26]. However, these studies did not explicitly address the influence of different curing conditions on the development of bond strength in early-age concrete. The novelty of this study lies in its comprehensive experimental and analytical investigation of the influence of curing conditions (moist curing vs. steam curing) on the early-age bond performance of GFRP-reinforced concrete [27]. In particular, this study provides new insights into the development of bond strength at early ages and proposes an analytical model that incorporates the effect of curing conditions to predict bond strength evolution. This approach addresses an important gap in the current literature and offers valuable guidance for the safe and efficient design of GFRP-reinforced concrete structures during the early stages of construction.

In this paper, a finite element analysis model using ABAQUS software is developed and applied in order to analyses the evolution of the thermal radial cracks in early age concrete according to the numerical model elaborated by Sdiri et al. [5]. Firstly, this model was developed to describe the thermo mechanical behavior of early age concrete using finite element analysis. On the other hand, it leads to model the early age concrete's cracking using the Mazars's damage Model [22]. Besides, the thermo-mechanical proprieties of early age concrete were implemented in this numerical model. Hymostrcut model [12] is used to determine the hydration degree variation of the simulated concrete. Furthermore, the thermal boundary condition is considered semi-adiabatic (20°C). Moreover, the analytical model developed by Zaidi et al. [20] will be applied for the early age concrete case study defining the concrete mechanical proprieties as functions of the hydration degree. As results, the variation of the radial thermal deformation as function of the time is deduced for the various temperature. The time's crack and the radial thermal concrete stress have been extracted from the results of the numerical simulations. The novelty of this work lies in its focus on the micro-mechanical implications of the curing process, offering new insight into how thermal and moisture gradients affect radial cracking and interfacial behavior in GFRP-reinforced systems. This approach fills a critical gap in current research, where curing effects are often overlooked in the assessment of concrete–GFRP performance.

2. HYDRATION PROCESS MODELING

2.1 Early age concrete modeling equations

This part deals with a finite element analysis of a GFRP reinforced early age concrete using ABAQUS software. The developed model is issued from an analytical study of Sdiri et al. [5]. In fact it describes the cement hydration process by taken in account the chimo-thermo-mechanical details (Table 1).

Table 1. Concrete mechanical proprieties [5, 20]

ρ	E_c	Gf	f_t	e	f=g	c	α
kg/m³	MPa	N/mm	MPa	-	-		10^{-5} (1/°C)
2400	40600	210	6,65	0.4	0,921	970	1

The studied element is considered as a prismatic concrete beam reinforced with 1HA25 GFRP rebar subjected to semi-adiabatic (20°C) thermal condition. The behavior of early-age concrete is modeled both numerically and analytically using a thermo-chemical-mechanical approach, which simulates the hydration process and incorporates the influence of the hydration degree (ξ) [5]. The rate of the hydration degree is expressed as follows:

$$\dot{\xi} = \frac{k}{n_0}\left(\frac{A_0}{k\xi_\infty} + \xi\right)(\xi_\infty - \xi)exp\,(-\frac{\bar{n}\xi}{\xi_\infty})\,exp\left(-\frac{Ea}{RT}\right) \qquad (1)$$

where, ξ is the concrete hydration degree, ξ_∞ presents the degree relatative to the finilization of the total hydration reactions. The chemical affinity A (in 1/h) characterizes the overall progression of each hydration reaction degree. n_0, $\bar{\mathbf{n}}$

are material constants, k is the thermal conductivity of the concrete. The concrete permeability η is directly linked with the microcirculation of the free water through the hydrates. ξ_∞ designs the final hydration degree. The Young's modulus $E_c(\xi)$, the compressive/tensile strength of concrete $f_{c,t}(\xi)$ and the fracture energy $Gf(\xi)$ depend on the degree of hydration according to the following:

$$\mathbf{f_{c,t}(\xi) = f_{c,}(\frac{\xi - \xi_0}{1 - \xi_0})^f} \quad (2)$$

$$\mathbf{E(\xi) = E_c(\frac{\xi - \xi_0}{1 - \xi_0})^e} \quad (3)$$

$$\mathbf{Gf(\xi) = Gf_c(\frac{\xi - \xi_0}{1 - \xi_0})^g} \quad (4)$$

where, $\boldsymbol{\xi_0}$ is the initial hydration degree.

The thermal strain in the concrete is expressed as follows:

$$\underline{\varepsilon}_{th} = \alpha \Delta T \quad (5)$$

where, α is the coefficient of the thermal expansion of the concrete.

The early age concrete cracks have been modeled referring to the Mazars damage model [5]. These model is defined as follows:

$$\mathbf{\underline{\sigma} = (1 - d)\underline{\underline{C}}\underline{\varepsilon}_{el}} \quad (6)$$

It should be noted that the Mazars damage model may present limitations when applied to early-age concrete reinforced with GFRP. The model does not explicitly account for the time-dependent evolution of mechanical properties due to hydration, which can affect both stiffness and damage development in the matrix. Additionally, the interaction between GFRP bars and the concrete matrix at early stages, where bond development is still progressing, may introduce discrepancies not captured by the isotropic damage framework. These factors can lead to deviations in predicted behavior, especially under early-age loading conditions. Recent studies, such as Li et al. [28] , have highlighted the importance of incorporating age-dependent material parameters or hybrid models to more accurately simulate the damage evolution in young, fiber-reinforced concrete.

The elastic strain tensor is computed as follows:

$$\underline{\varepsilon}_{el} = \underline{\varepsilon} - \underline{\varepsilon}_{th} \quad (7)$$

The damage variable

$$d = 1 - \frac{\varepsilon_{d0}}{\tilde{\varepsilon}} exp(\frac{l_c f_t}{G_f}(\varepsilon_{d0} - \tilde{\varepsilon})) \text{ [5]} \quad (8)$$

$$\tilde{\varepsilon} = \sqrt{\langle \varepsilon_e{}^I \rangle^2 + \langle \varepsilon_e{}^{II} \rangle^2 + \langle \varepsilon_e{}^{III} \rangle^2} \quad (9)$$

$$\varepsilon_{d0} = \frac{f_t(\xi)}{E(\xi)} \quad (10)$$

where, ε_{d0} is the damage threshold. $\tilde{\varepsilon}$ is defined as the equivalent strain, $\langle \varepsilon_e{}^I \rangle$, $\langle \varepsilon_e{}^{II} \rangle$ and $\langle \varepsilon_e{}^{III} \rangle$ are the positive parts of the elastic strain eigenvalues.

The thermomechanical model described is numerically integrated using the finite element software ABAQUS, with the development of three user subroutines: HETVAL, UEXPAN, and UMAT [5]. The HETVAL subroutine is used to model the internal hydration heat flux. Following this, the thermal and shrinkage strains are integrated within the UEXPAN subroutine. The total strain is then calculated by incorporating these effects. Once the increment in eigen strain is determined, both the mechanical strain increment and the current mechanical strain are computed. These values are subsequently used as inputs in the UMAT user-material subroutine. This allows for the calculation of the early-age concrete's mechanical properties based on the explicit degree of hydration. The numerical implementation of the thermochemical model is more detailed in Sdiri et al. [5] paper.

$$\xi_{n+1} - \xi_n - \frac{k}{n_0}\left(\frac{A_0}{k\xi_\infty} + \xi_{n+1}\right)(\xi_\infty - \xi_{n+1}) exp\left(-\frac{\bar{n}\xi_{n+1}}{\xi_\infty}\right) exp\left(-\frac{Ea}{R\,T_{n+1}}\right) = 0 \quad (11)$$

Sdiri et al. [5] provides a comprehensive overview of the mechanisms behind early-age cracking in restrained concrete elements.

2.2 Analytical study of hardened concrete

For the GFRP reinforced concrete element, rebars generates local radial pressure at the bar / concrete interface especially when the local temperature increases. Thus, the hydration temperature may lead to the appearance of such thermal stress. Subsequently, early age concrete radial crack appears. Zaidi et al. [20] developed an analytical study that treat the radial concrete crack formation at hardening stage. The specimen model is considered as a cylindrical concrete specimen reinforced centrally by a GFRP rebar (Figure 1). Table 2 illustates the concrete speciemen dimensions.

Table 2. Glass fiber reinforced polymer (GFRP) rebars mechanical and physical proprieties [20]

Bar Diameter Φ (mm)	Concrete Diameter (D) (mm)	Concrete Length L (mm)	Rebar Length (mm)
25,4	76	380	400

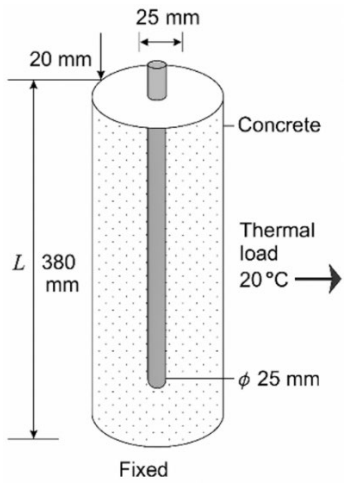

Figure 1. Concrete model [20]

Only thermal load are applied and the following conditions are taken in account:

1- A perfect bond is assumed between the GFRP bar and the surrounding concrete.
2- Both the GFRP bar and the concrete exhibit linear elastic behavior.
3- The cross-section of the cylinder remains plane after thermal deformation.

According to Zaidi et al. [20], the radial thermal deformation relative to hardened concrete is defined as follows ε_{ct}:

$$\varepsilon_{ct} = \frac{P}{\mathrm{E}}\left(\frac{r^2+1}{r^2-1}+\nu\right)+\alpha_b \Delta T \tag{12}$$

where, $r = \frac{\Phi_c}{\Phi_r}$, Φ_r the bar diameter, Φ_c concrete cylindrical element diameter and ν is the concrete Poisson ratio. The radial pressure P excreted by the GFRP at the around concrete is induced mainly by the temperature variation as expressed in the following formula:

$$P = \frac{(\alpha_R - \alpha)\Delta T}{\frac{1}{\mathrm{E}}\left(\frac{r^2+1}{r^2-1}+\nu\right)+\frac{(1-v_A)}{E_R}} \tag{13}$$

where, α_R is the GFRP radial thermal expansion coefficient. v_A is the GFRP axial coefficient ration and E_T is the E_R is the radial elastic modulus of the GFRP rebar.

The maximum circumferential stress $\boldsymbol{\sigma_{t\,max}}$ generated by the radial pressure is expressed as follows:

$$\boldsymbol{\sigma_{t\,max}} = \frac{\boldsymbol{r^2+1}}{\boldsymbol{r^2-1}}\boldsymbol{P} \tag{14}$$

In order to predict the concrete radial crack formation, the analytical model of Zaidi et al. [20] has been applied on the early age stage. In fact, the constituve equations of the thermal radial cracks, the radial pressure and concrete tensile strength depend on the mechanical proprieties of the concrete. Hence, it can be expressed as functions of the hydration degree ξ according to the formula of De Schutter and Taerwe [13].

$$P\,(t) = \frac{(\alpha_{PRFV} - \alpha)\Delta T}{\frac{1}{\mathrm{E}(\xi(t))}\left(\frac{r^2+1}{r^2-1}+\nu\right)+\frac{(1-v_A)}{E_t}} \tag{15}$$

$$\varepsilon_{ct}(t) = \frac{P(\xi(t))}{\mathrm{E}(\xi(t))}\left(\frac{r^2+1}{r^2-1}+\nu(\xi(t))\right)+\alpha\Delta T \tag{16}$$

$$\sigma_{t\_max}(t) = \frac{r^2+1}{r^2-1}P(\xi(t)) \tag{17}$$

3. NUMERICAL SIMULATIONS

3.1 Material proprieties

(a) Concrete

The concrete used in this study is ordinary concrete, characterized by the mechanical properties listed in Table 1. These data are taken from the experimental campaign carried out by Zaidi et al. [20]. The concrete is considered as elastic undamageable material.

To assess the variation in the degree of hydration of the concrete used, an approximate simulation was conducted using Hymostruct, based on standard cement compositions [21] (Table 3).

The results of the simulation are resumed in Figure 2. The hydration degree increases with the concrete age until it attempts a final hydration degree equal to ξ_∞=0,69. The missing hydration model parameters are identified according Sdiri et al [5]. These parameters depend mainly on the concrete proprieties. The chemical hydration parameters are summarized in Table 4, which presents the initial and final values of the hydration degree.

Figure 2 shows a rapid increase during the early hours, followed by a gradual slowdown, indicating the typical progression of cement hydration.

(b) GFRP rebars

The GFRP mechanical proprieties are detailed in Table 5.

Table 3. Chemical compositions of cement [21]

Cement Compost	CaO	SiO_2	Al_2O_3	Fe_2O_3	K_2O	Na_2O	SO_3	TiO_2	P_2O_5
Percentage %	63	22	4,96	3	0,64	0,14	2,57	0,35	0,18

Table 4. Hydration parameters [5]

ξ_0	ξ_∞	$\frac{k}{n_0}$	$\frac{Ea}{R}$	$\bar{n}$
0,1	0,69	**1.05×10^7**	5000	3,39

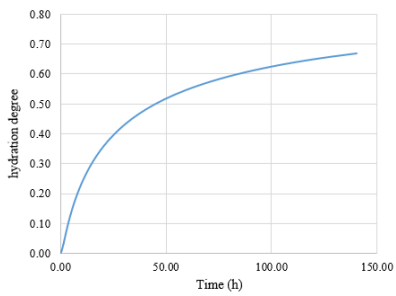

Figure 1. Hydration degree variation as function of time

Table 5. GFRP rebars mechanical and physical proprieties [20]

Bar Diameter (mm) Φ	E_A (GPa)	E_R (GPa)	ν_A	ν_R	α_A (×10^{-5} 1/°C)	α_R (×10^{-5} 1/°C)
25,4	42	7,1	0,28	0,38	0,6	2,2

3.2 Model description

The concrete element was modeled using the finite element software ABAQUS, as illustrated in Figure 3. It is represented as a cylindrical specimen reinforced with a GFRP rebar. For both the concrete and the reinforcement, C3D8T coupled temperature-displacement elements were employed [5]. The characteristics of the cylindrical element (diameter, concrete cover, embedded length) are presented in the study work of Zaidi et al. [20]. These properties are summarized in the following table. A semi-adiabatic thermal condition at 20°C is assumed. The study focuses on the free thermal behavior; therefore, the mechanical boundary conditions are considered free at the transverse sections of both the concrete and the GFRP rebar.

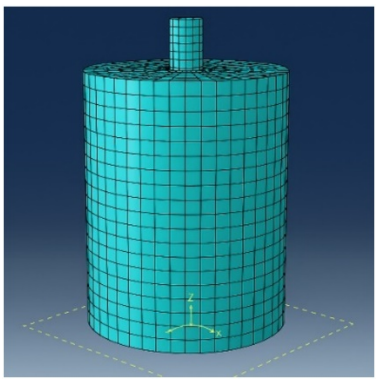

Figure 3. Modelled reinforced concrete element

4. RESULTS

4.1 Model validation

Figure 4 describes the temperature variation as function of the concrete age for a temperature of $T_0 = 20°C$ and GFRP diameter Φ=25,4 mm. It can be deduced that early age concrete reaches a maximum temperature $T_{max} = 50°C$ at the age of 20 hours. This behavior highlights the exothermic nature of the hydration process. After approximately 20 hours, the temperature begins to decrease, eventually returning to its initial level.

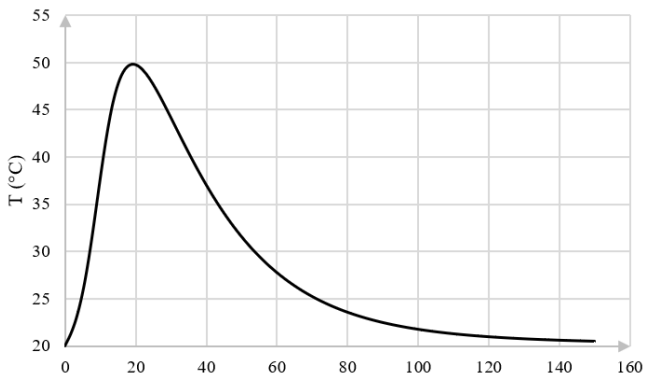

Figure 4. Concrete temperature variation as function of time

For the same tested specimen, the radial thermal deformation ε_{ct} has been determined at the interface between the GFRP rebar and early-age concrete using two different approaches: (i) the analytical expression developed by Zaidi et al. [20] (Eq. (12)), and (ii) the results obtained from the ABAQUS FE numerical simulation. The numerical curve was extracted at a node located directly at the GFRP–concrete interface. As illustrated in Figure 5, the analytical curve demonstrates strong agreement with the numerical results, validating the proposed model. To further quantify this agreement, statistical error analysis was conducted. The deviation between the analytical and numerical results was assessed using three standard metrics:

- Mean absolute error (MAE)

$$MAE = \frac{1}{N}\sum_{i=1}^{N}\left|\varepsilon_{ct,i}^{analytical} - \varepsilon_{ct,i}^{numerical}\right| \quad (18)$$

- Root mean square error RMSE

$$RMSE = \sqrt{\frac{1}{N}\sum_{i=1}^{N}\left(\varepsilon_{ct,i}^{analytical} - \varepsilon_{ct,i}^{numerical}\right)^2} \quad (19)$$

with N= 50 (the data numbers).

The statistical error analysis confirms that the analytical expression for the radial thermal deformation developed by Zaidi et al. [20] is highly accurate and in good agreement with the results obtained from the ABAQUS finite element simulation. The use of the three error metrics absolute error, relative error, and RMSE has quantitatively demonstrated the robustness of the analytical model, supporting its application for further studies on GFRP-reinforced concrete structures.

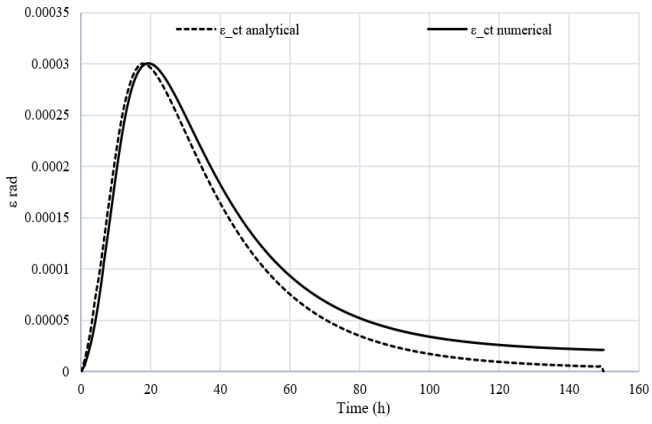

Figure 5. Radial thermal crack at early age concrete

The computed values for the current study are:

$MAE = 8.57 \times 10^{-6}$ and RMSE $= 8.86 \times 10^{-6}$, confirming a very close match between both approaches. Moreover, the maximum radial strain deformation occurs at approximately 20 hours, which coincides with the time when the concrete reaches its peak temperature (Tmax=50°C). This behavior highlights the influence of the thermal gradient

generated by the hydration process, which acts as a transient thermal load applied to the concrete specimen [23].

4.2 Radial crack distribution

For a specimen reinforced with a GFRP rebar of Φ= 25mm, Figure 6 describes the damage distributions at the GFRP/concrete interface for different ages of the concrete 5 hours, 10 hours and 20 hours. It is shown that the damage increases with the age of the concrete, reaching its maximum at around 20 hours. This corresponds to the time when the concrete reaches its peak temperature t = 20 hours, $T_{max} = 50\ °C$.

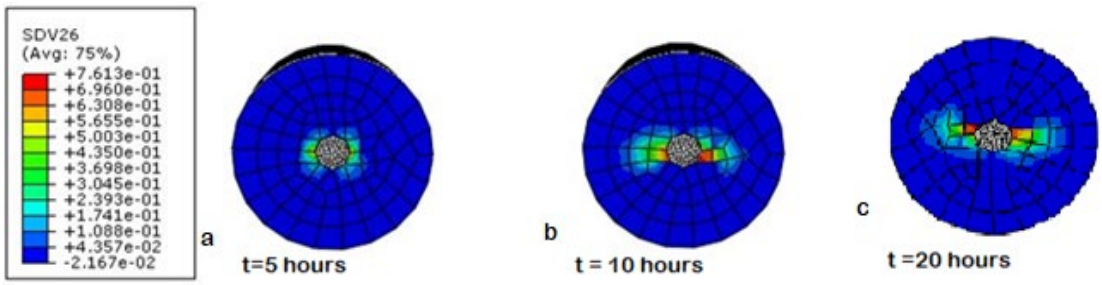

Figure 6. Radial crack distribution at GFRP reinforced concrete element at t=5, 10 and 20 hours

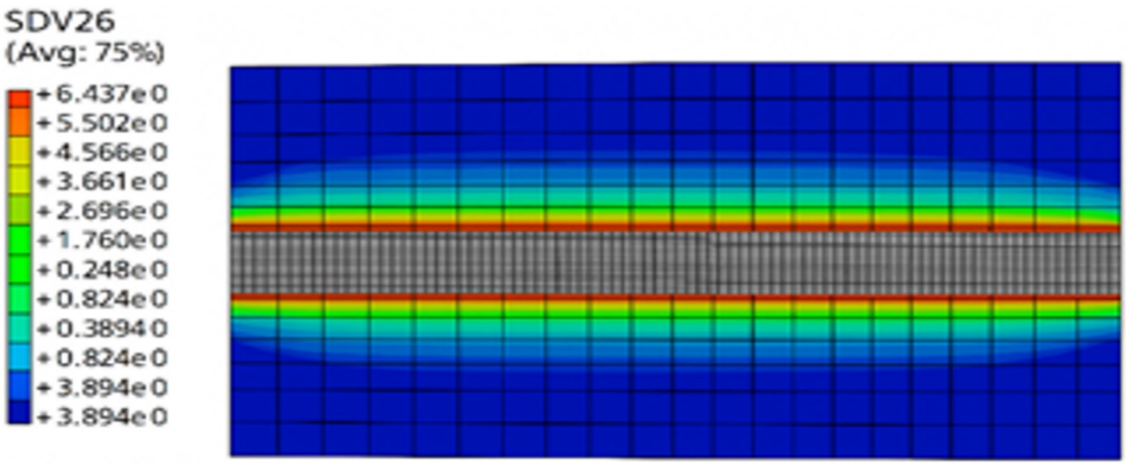

Figure 7. Radial crack distribution at GFRP reinforced concrete element at t=20 hours

Figure 7 presents the longitudinal crack distributions for the concrete specimen at 20 hours from the concrete ages. According to the hydration degree variation (Figure 2), the hydration degree relative to the concrete's age t=20 hours is equal to $\xi = 0.48$. The radial pressure relative to this hydration degree is calculated according to Eq. (20).

$$P\ (\xi = 0.48) = \frac{(\alpha_r - \alpha_c)\Delta T(\xi = 0.48)}{\frac{1}{\mathrm{E}(\xi = 0.48)}\left(\frac{r^2+1}{r^2-1} + \nu_c\right) + \frac{(1-\nu_A)}{E_A}} \quad (20)$$

where, $\mathrm{E}(\xi = 0.48)$ is calculated according to Eq. (3). The calculated radial pressure.

$P(\xi = 0.48) = 4{,}11$ MPa . As results, the early age circumferential radial stress is determined according to Eq. (17). $\sigma_{t\,max} = 5{,}58\,MPa$. At the same concrete age, the concrete tensile strength is calculated as function of the hydration degree by referring to Eq. (2). $ft(\xi = 0.48) = 5\,MPa$. As results, it can be noted that the concrete stress reaches the tensile strength: this explains the presence of cracks in concrete around the GFRP reinforcement. Furthermore, this is due to the attempt of the maximum temperature of the hydration process and the variation of the radial thermal coefficient (CET) of both the concrete and the GFRP one. As results, the hydration temperature evolution presents a major factor of the appearance of thermal cracks at early age concrete not only for the hardened one. Furthermore, it is more pronounced by the difference between the GFRP radial thermal coefficient and its similar of the concrete.

5. CONCLUSIONS

In this paper, a finite element and analytical analysis of the thermal radial crack evolution at a GFRP early age concrete reinforced element has been carried out. The numerical and analytical analysis is developed by Sdiri et al [5]. The crack is modeled using the Mazars damage analytical model. Only thermal strain has been taken in account. At first, the hydration evolution has been determined using Hymostruct procedure according to the cement chemical compositions. Hence, the hydration degree variation has been determined as function of the time. Subsequently, the final hydration degree of the used concrete is determined. The radial crack formation for hardened concrete is described by ana analytical study elaborated by Zaidi et al. [20]. In fact, the difference between

the radial thermal expansion coefficient of the GFRP rebar and its similar of the concrete has been taken in account to evaluate analytically the radial thermal strain, the radial pressure applied by the concrete on the GFRP rebar. The maximum concrete strength is also deduced analytically. In order to prevent the radial crack formation at early age stage, the mechanical proprieties of the concrete, like the elastic modulus and the tensile strength, have been expressed as functions of the hydration degree according to the model of Sdiri et al. [5]. Numerical simulation using ABAQUS software is applied on a cylindrical GFRP reinforced element. The following results were achieved from the numerical simulation:

- The early age concrete attempts a maximum temperature of 50°C caused by the hydration process.
- The analytical model is well validated according to the numerical variation of the radial crack strain: The strain reaches its maximum at the age of 20 hours: this age is relative to the maximum hydration concrete temperature: this temperature variation replaces the thermal load effect modelled at the hardened concrete case study.
- At the age of 20 hours, the concrete tensile strength is calculated according to De Schutter expression and the relative hydration degree is deduced from Hymostruct results: the radial pressure, the maximum radial stress was calculated and compared to the associated tensile strength: it reaches its value and this explains the presence of the radial crack at the concrete.
- The radial damage repartitions are extracted for different concrete ages 5 hours, 10 hours and 20 hours: it is noted that the crack formations were developed speedily as function of concrete age.

It is acknowledged that the present study did not include microstructural analysis of the cracked concrete specimens. Incorporating such analysis in future research would provide further insight into the damage mechanisms at the micro-level and enhance the understanding of the interaction between cracks and the surrounding cementitious matrix. Besides, this study presented a numerical investigation into the effect of curing conditions on radial damage development in GFRP-reinforced concrete. The results demonstrated that steam curing, although beneficial for accelerating early strength development, can increase the risk of localized damage due to thermal stresses around the GFRP reinforcement. In contrast, hydration curing resulted in more uniform stress distribution and reduced damage concentration. These findings have practical implications for structural engineering design. Specifically, they suggest that hydration curing may be more suitable for structures where long-term durability and crack control around GFRP bars are critical. Moreover, the results highlight the importance of selecting GFRP reinforcement with appropriate thermal and mechanical properties when used in high-temperature curing environments. These insights provide a foundation for optimizing curing protocols and reinforcement selection to improve the performance and longevity of GFRP-reinforced concrete elements, especially in precast or thermally cured structural applications.

REFERENCES

[1] Smolana, A., Klemczak, B., Azenha, M., Schlicke, D. (2022). Thermo-mechanical analysis of mass concrete foundation slabs at early age—Essential aspects and experiences from the FE modelling. Materials, 15(5): 1815. https://doi.org/10.3390/ma15051815

[2] Zhao, K., Zhang, P., Xue, S., Han, S., Mueller, H.S., Xiao, Y., Li, Q. (2021). Quasi-elastic neutron scattering (QENS) and its application for investigating the hydration of cement-based materials: State-of-the-art. Materials Characterization, 172: 110890. https://doi.org/10.1016/j.matchar.2021.110890

[3] Pang, X., Sun, L., Sun, F., Zhang, G., Guo, S., Bu, Y. (2021). Cement hydration kinetics study in the temperature range from 15°C to 95°C. Cement and Concrete Research, 148: 106552. https://doi.org/10.1016/j.cemconres.2021.106552

[4] Joseph, S., Cizer, Ö. (2022). Hydration of hybrid cements at low temperatures: A study on portland cement-blast furnace slag—Na_2SO_4. Materials, 15(5): 1914. https://doi.org/10.3390/ma15051914

[5] Sdiri, A., Kammoun, S., Daoud, A. (2021). Numerical modeling of the interaction between reinforcement and concrete at early age—A comparison between glass fiber reinforced polymer and steel rebars. Structural Concrete, 22(1): 168-182. https://doi.org/10.1002/suco.201900314

[6] Liang, T., Luo, P., Mao, Z., Huang, X., Deng, M., Tang, M. (2023). Effect of hydration temperature rise inhibitor on the temperature rise of concrete and its mechanism. Materials, 16(8): 2992. https://doi.org/10.3390/ma16082992

[7] Emmanuel, A.C., Krishnan, S., Bishnoi, S. (2022). Influence of curing temperature on hydration and microstructural development of ordinary Portland cement. Construction and Building Materials, 329: 127070. https://doi.org/10.1016/j.conbuildmat.2022.127070

[8] Smolana, A., Klemczak, B., Azenha, M., Schlicke, D. (2021). Early age cracking risk in a massive concrete foundation slab: Comparison of analytical and numerical prediction models with on-site measurements. Construction and Building Materials, 301: 124135. https://doi.org/10.1016/j.conbuildmat.2021.124135

[9] Safiuddin, M., Kaish, A.A., Woon, C.O., Raman, S.N. (2018). Early-age cracking in concrete: Causes, consequences, remedial measures, and recommendations. Applied Sciences, 8(10): 1730. https://doi.org/10.3390/app8101730

[10] Shen, M., Zhao, Y., Bi, J., Wang, C., Du, B. (2024). Microstructure evolution and damage mechanisms of concrete-rock-composite corrosion in acid environment. Journal of Building Engineering, 82: 108336. https://doi.org/10.1016/j.jobe.2023.108336

[11] Ye, G., Van Breugel, K., Fraaij, A.L.A. (2003). Three-dimensional microstructure analysis of numerically simulated cementitious materials. Cement and Concrete Research, 33(2): 215-222. https://doi.org/10.1016/S0008-8846(02)00889-X

[12] Bentz, D.P. (2000). CEMHYD3D: A three-dimensional cement hydration and microstructure development modelling package. International Journal of Advanced Engineering Sciences and Applied Mathematics, 2: 75-82.

[13] De Schutter, G., Taerwe, L. (1996). Degree of hydration-based description of mechanical properties of early age concrete. Materials and Structures, 29: 335-344. https://doi.org/10.1007/BF02486341

[14] Alsuhaibani, E., Alturki, M., Alogla, S.M., Alawad, O., Alkharisi, M.K., Bayoumi, E., Aldukail, A. (2024). Compressive and bonding performance of GFRP-reinforced concrete columns. Buildings, 14(4): 1071. https://doi.org/10.3390/buildings14041071
[15] Rasheed, M.R., Mohammed, S.D. (2024). Structural behavior of concrete one-way slab with mixed reinforcement of steel and glass fiber polymer bars under fire exposure. Engineering, Technology & Applied Science Research, 14(2): 13380-13387.
[16] Manoj, T., Mrudhul varma, B., Seshagiri rao, M.V. (2023). Performance evaluation of conventional and lightweight concrete using GFRP sheets at elevated temperature. Materials Today: Proceedings. https://doi.org/10.1016/j.matpr.2023.05.115
[17] Zhang, F., Lu, Z., Wang, D. (2024). Working and mechanical properties of waste glass fiber reinforced self-compacting recycled concrete. Construction and Building Materials, 439: 137172. https://doi.org/10.1016/j.conbuildmat.2024.137172
[18] Rawat, P., Singh, K.K., Singh, P.K. (2020). Comparison of steel and fiber-reinforced polymer rebars for mining applications: A numerical approach. Materials Today: Proceedings, 33: 5041-5045. https://doi.org/10.1016/j.matpr.2020.02.840
[19] Blaznov, A.N., Krasnova, A.S., Krasnov, A.A., Zhurkovsky, M.E. (2017). Geometric and mechanical characterization of ribbed FRP rebars. Polymer Testing, 63: 434-439. https://doi.org/10.1016/j.polymertesting.2017.09.006
[20] Zaidi, A., Masmoudi, R., Bouhicha, M. (2013). Numerical analysis of thermal stress-deformation in concrete surrounding FRP bars in hot region. Construction and Building Materials, 38: 204-213. https://doi.org/10.1016/j.conbuildmat.2012.08.047
[21] Dunuweera, S.P., Rajapakse, R.M.G. (2018). Cement types, composition, uses and advantages of nanocement, environmental impact on cement production, and possible solutions. Advances in Materials Science and Engineering, 2018(1): 4158682. https://doi.org/10.1155/2018/4158682
[22] Benmokrane, B., Elgabbas, F., Ahmed, E.A., Cousin, P. (2015). Bond behavior of glass fiber-reinforced polymer (GFRP) bars in self-consolidating concrete. ACI Materials Journal, 112(2): 231-240.
[23] Lei, Z., Luo, J., Zhang, S., Wang, E., Huang, H. (2024). Mechanical properties of GFRP bars exposed to natural erosion environment: A case study. Case Studies in Construction Materials, 21: e03734. https://doi.org/10.1016/j.cscm.2024.e03734
[24] Tarabin, M., Maalej, M., Altoubat, S., Junaid, M.T. (2023). Review of the bond behavior between reinforcing steel and engineered cementitious composites. Structures, 55: 2143-2156. https://doi.org/10.1016/j.istruc.2023.07.025
[25] Hossain, K.M.A. (2018). Bond strength of GFRP bars embedded in engineered cementitious composite using RILEM beam testing. International Journal of Concrete Structures and Materials, 12: 6. https://doi.org/10.1186/s40069-018-0240-0
[26] Bediwy, A.G., El-Salakawy, E.F. (2021). Bond behavior of straight and headed GFRP bars embedded in a cementitious composite reinforced with basalt fiber pellets. Journal of Composites for Construction, 25(5): 04021038. https://doi.org/10.1061/(ASCE)CC.1943-5614.0001147
[27] Roghani, H., Nanni, A., Bolander, J.E. (2023). Early-age cracking behavior of concrete slabs with GFRP Reinforcement. Materials, 16(15): 5489. https://doi.org/10.3390/ma16155489
[28] Li, B., Chen, Z., Wang, S., Xu, L. (2024). A review on the damage behavior and constitutive model of fiber reinforced concrete at ambient temperature. Construction and Building Materials, 412: 134919. https://doi.org/10.1016/j.conbuildmat.2024.134919

NOMENCLATURE

GFRP	Glass fiber reinforced polymer
CET	Coefficient of thermal expansion
E_c	Concrete elastic modulus, (MPa)
E_A	GFRP axial elastic modulus, (MPa)
E_r	GFRP radial elastic modulus, (MPa)
P	Radial Pression of FRP rebar on concrete, (MPa)
G_f	Concrete fracture energy, (N/mm)
f_t	Concrete tensile strengh, (MPa)
ΔT	Temperature variation, (°C)
T	Temprature, (°C)
T_n	Temprature relative to time (tn), (°C)
C	Elastic matrix
MAE	Mean absolute error
RMSE	Root mean square error

Greek Symbols

α_A	GFRP axial thermal expansion coeffcient, (1/°C)
α_r	GFRP Radial thermal expansion coeffcient, (1/°C)
$\varepsilon_{ct,i}^{analytical}$	Analytical thermal strain
$\varepsilon_{ct,i}^{numerical}$	Numerical thermal strain
ξ	Hydration degree
ξ_0	Intial hydration degree
ξ_∞	Final hydration degree
ξ_n	Hydration degree relative to time (n)
$\sigma_{t\,max}$	Maximum thermal circofrentiel stress on concrete, (MPa)
$\underline{\sigma}$	Stress matrix
$\underline{\varepsilon}$	Strain matrix
ε_{ct}	Thermal radial strain
k	Thermal conductivity of the concrete
η	The concrete permeability
ν_c	Poission ratio of concrete
ν_A	GFRP axial Poission ratio
ρ	Concrete Density, (kg/m^3)